

**How to Cite:**

Bhat, M. R., Salroo, I. N., & Ahmad Mir, R. (2022). Hemodynamic evaluation of coarctation of aorta using phase: Contrast magnetic resonance imaging and its comparison with echocardiographic findings evaluation of coarctation of aorta. *International Journal of Health Sciences*, 6(S1), 12365–12382. <https://doi.org/10.53730/ijhs.v6nS1.8083>

# **Hemodynamic evaluation of coarctation of aorta using phase – Contrast magnetic resonance imaging and its comparison with echocardiographic findings evaluation of coarctation of aorta**

**Musaddiq Rafiq Bhat**

Senior Resident, Department of Radiodiagnosis & Imaging, SKIMS Medical College, Srinagar, J&K, India.

Email: [drmusaddiqrafiqbhat@gmail.com](mailto:drmusaddiqrafiqbhat@gmail.com)

**Imran Nazir Salroo**

Assistant Professor, Department of Radiodiagnosis & Imaging, SKIMS Medical College, Srinagar, J&K, India.

Email: [imransalroodr@gmail.com](mailto:imransalroodr@gmail.com)

**Reyaz Ahmad Mir**

Senior Resident, Department of Radiodiagnosis & Imaging, SKIMS Medical College, Srinagar, J&K, India.

Corresponding Author Email: [mirreyaz212@gmail.com](mailto:mirreyaz212@gmail.com)

**Abstract**---Background: Coarctation of aorta (CoA) occurs when a small section of the aorta narrows in the luminal. CoA is one of the most popular congenital CL (cardiac lesions), and it is responsible for five to ten percent of all instances of congenital HD (heart disease). CoA can result in a variety of complications. Aims & Objectives: This research was undertaken to determine the occurrence of related CL and valvular disorders in patients with CoA. Materials and Methods: This research was carried out in the Department of Radiodiagnosis and Imaging (DORAI), Sher-i-Kashmir Institute of Medical Sciences (SKIMS) Tertiary Care Hospital, Srinagar, JK, India over a period of 2 years on patients referred from the Department of Cardiology. The patients who had been detected with CoA were given a PC-MRI to check their blood flow, and the comparison was made to the Echocardiographic study results. Results: Spin-echo (S-E) images of the level of the aortic arch (AA) as well as aortic isthmus (AI) showed narrowing in nineteen situations, according to the researchers. In

eleven of the twenty situations, there was a significant amount of collateral circulation (CC). CC was significant in six out of eleven situations of serious stenosis. There was significant CC in three of the five situations of moderate stenosis. One situation had tubular hypoplasia of the AA; two situations had PFO; one situation had Shone complex; and one situation had pseudo-coarctation of the aorta ( $\Delta p=12\text{mm Hg}$ ). Doppler echocardiography (DE) was used to diagnose coarctation in seventeen of the twenty patients, and concern of coarctation and/or AA hypoplasia was brought up in three situations. Conclusion: There was perfect correlation for the delineation of spectrum of associated anomalies between ECHO-MTD, ECHO-MRI, and MRI- MTD.

**Keywords**---ECHO, Doppler, Coarctation, Aorta, MRI.

## Introduction

CoA occurs when a small section of the aorta narrows in the luminal<sup>1</sup>. CoA is one of the most popular congenital CL, and it is responsible for five to ten percent of all instances of congenital HD. Even though congenital HD is relatively uncommon, it affects eight out of every one thousand births. Due to the success of medical or surgical treatment in children, the number of people who have it has grown<sup>1</sup>. Most of the time, CoA happens where the DA (ductus arteriosus)<sup>2-4</sup> connects to the left subclavian artery. This is considered to be because the DT (ductal tissue) around the AI (aortic isthmus)<sup>5</sup> contracts too much at birth, when the DA also contracts.

CoA can lead to many complications such as neonatal heart failure, subarachnoid hemorrhage, aortic dissection, infective endocarditis and mycotic aneurysm<sup>6</sup>. Moreover, CoA can be evaluated by plain radiography, electrocardiogram, antenatal ultrasound and echocardiography<sup>6,7</sup>. Coarctation is an ailment that is often not diagnosed early, and when it isn't caught early, it takes longer to treat. If treatment is delayed, the coarctation's effects will worsen, increases the risk for heart attacks and sudden deaths<sup>8</sup>. About twenty-five percent of people die from a ruptured aorta, twenty percent die from infected aortitis or endocarditis, twenty percent die from cardiac failure, ten percent die from severe bleeding in brain, and ten percent die from a ruptured heart (around one percent)<sup>9</sup>. A wide range of clinical as well as radiological imaging methods are used in the treatment of coarctation in light of the above limitations and the importance of early detection. The diagnostic armamentarium for CoA has developed over time, beginning with the determination of pressure differences between both the lower & upper extremities as well as clinical findings like cardiac murmurs. Imaging therapies, on the other hand, have increased our understanding of the accurate scanning of this condition.

This research was performed to see the evaluation of related CL or VA (valvular affections) in patients with CoA and mapping of collaterals, measuring pressure gradients (PG) by means of Phase-Contrast MRI, as well as comparison of MRI findings with echocardiographic findings and catheter angiography findings.

## Material and Methods

This research was undertaken in the DORAI, SKIMS in Srinagar, JK, India. This research was carried out for two years on patients referred from the Department of Cardiology, SKIMS Soura, Srinagar. The patients who had been detected with CoA were subjected to a haemodynamic assessment using a PC-MRI scanner, and the comparison is made to those obtained from Echocardiography.

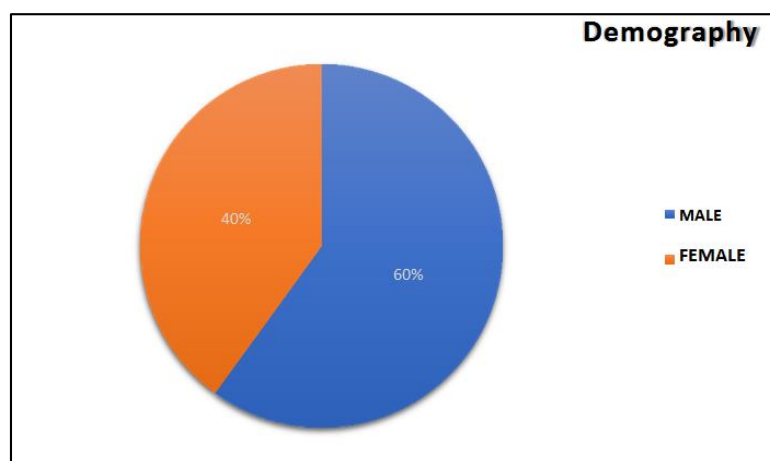


Figure 1. Demographic Composition of our study

The research involved all patients who were diagnosed with CoA based on echocardiographic research results. Criteria for exclusion comprised patients detected with CoA via echocardiography who had contraindications for Cardiac-MRI (such as heavy metal foreign bodies, non-MR suitable pacemakers or metallic prosthesis).

Trans-thoracic echocardiography (TTE) was conducted through “GE Vivid E95 Echocardiography System” by professionals with minimum five to ten years of experience in Echocardiography. TTE was performed through parasternal, apical, subxiphoid, as well as suprasternal methods, and an apical four-chamber view, tract view of RV (right ventricular) outflow, and long-axis view of LV (left ventricular).

After that, a Phase-contrast MRI study was done on all these patients through a 1.5-T MRI machine (Siemens Medical System, Erlangen, Germany). Then, the cine-MR imaging was done using the pulse sequences of segmented fast field echo (FFE) and gradient-echo (GE) that had already been found. Sixteen to twenty-five frames were shown in a cine loop to provide a flexible approach to the cardiac cycle. It was done in all situations using an oblique sagittal plane (OSP) that encompassed the AA, which was supported by an oblique coronal plane (OCP) that was primarily focused on the AI. The narrowing caused by the coarctation was measured using the images of diastolic. As the coarctation was contacted, systolic images related to the blood pool were taken at the level as well as below the coarctation to demonstrate the void caused by turbulence as well as acceleration off low.

The pressure gradient all over coarctation was then measured using the images of velocity-encoded cine MR (VENC-MRI). We also did MRI (MR imaging) with phase contrast on these people. ARGUS software was used to perform flow as well as velocity measurements on the PC-MR images that were collected through this manner.

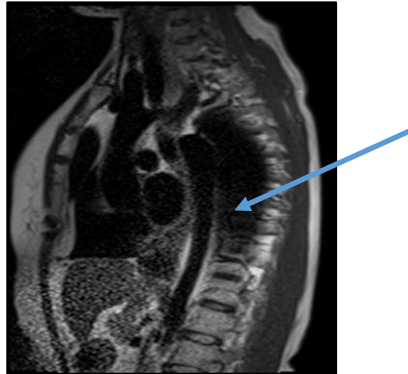


Figure 2. MR image of Phase Contrast in OSP with severe coarctation in a patient

Aliasing can be seen in the phase image when the VENC is low (curved arrow). When the encoding velocity ( $V_{MAX}$ ) is positioned correctly, aliasing in the stenotic jet disappears as the VENC value rises (arrow).

In order to determine the gradient of the coarcted segment, we used the equation:

$$\Delta p = 4 \cdot (V_{max})^2.$$

To produce accurate PG, which has a dimension in millimetres of mercury,  $V_{max}$  must have a dimension of metres per second (mm Hg).

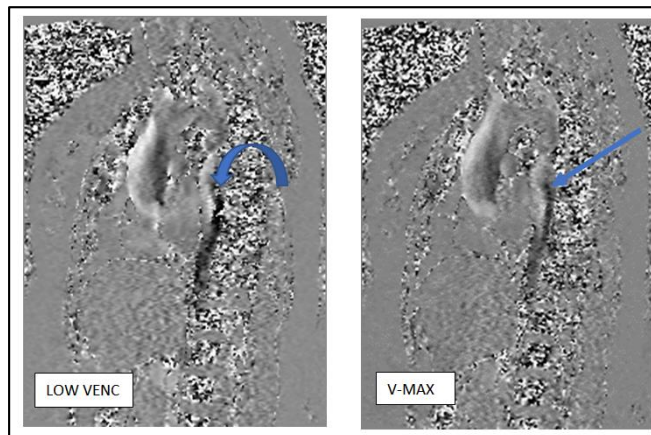


**Figure 3.** MR image of Phase Contrast in OSP with severe coarctation in a patient

Aliasing can be seen in the phase image when the VENC is low (curved arrow). When the encoding velocity ( $V_{MAX}$ ) is positioned correctly, aliasing in the stenotic jet disappears as the VENC value rises (arrow). In some patients, 3-dimensional CEMRA was done after a small examination bolus injection of Gadolinium (two millilitres) to find out when the comparison got to the TA (thoracic aorta).

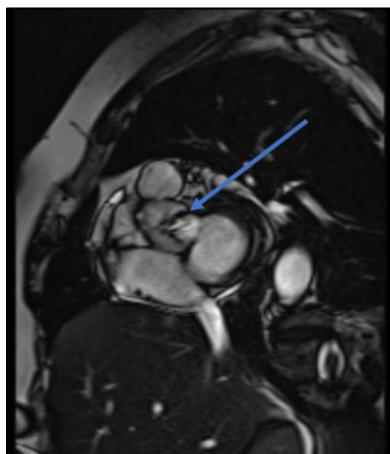


**Figure 4.** Image of the whole TA and the CoA can be obtained using gadolinium-enhanced MR angiography (arrow). They are effective for displaying CC also (curved arrow)

**Severity of CoA:** The coarctation length was viewed short. This arises when the narrowed aortic segment length was less than 0.5 centimetres and long if it was greater than 0.5 centimetres<sup>10</sup>. It was assumed that the AA was hypoplastic whenever the transverse diameter ratio was below 0.90 as compared to the distal DA (descending aorta) diameter.<sup>11</sup> 2 experienced & skilled radiologists measured the internal blood vessels diameters using S-E, cine, or CEMRA source along with the images of reconstruction and therefore showed the good image of the entire segment of lumen. The subclavian artery and the left common carotid were compared to determine the AA's diameter. The origin of the subclavian artery's diameter was assessed. The smallest inner diameter of the constricted segment was shown and compared to the diameter of the DA end to determine the isthmus coarctation (IC). The first centimetres of the thoracic DA were evaluated for post-stenotic aortic diameter.

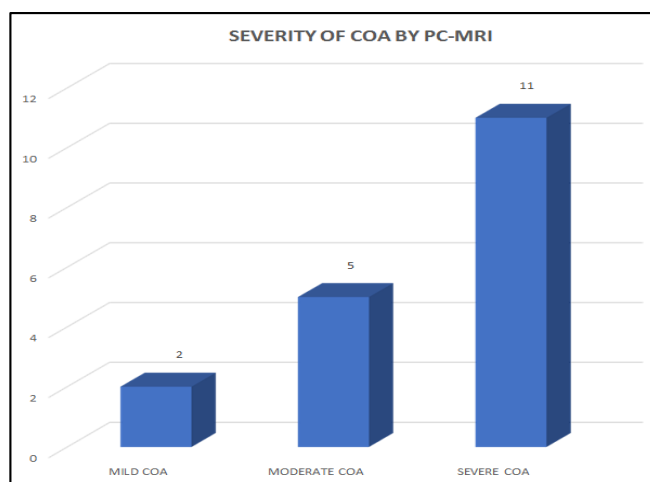


**Figure 5.** Graphical depiction of PC-MRI which showed the number of incidents of mild, moderate, & severe CoA

All of the patients in this group had their morphologic MR observations especially in comparison to their Doppler echocardiography (DE) outcomes. In fifteen situations, the outcomes of VENC MR Sequences were contrasted with the findings of DE. This is done to get an idea of how the pressure changes across the coarctation. The analysis of image also included the detection of related anomalies such as ASD, VSD, PDA, BAV, LVH, PAH, and aortic side branch deformities.

Table 1  
Comparison of ASD, VSD, PDA, and LVH detected by Echo, MRI and MTD

ASD	ECHO-MTD	ECHO-MRI	MRI-MTD
Kappa	0.773	1	0.773
Level of agreement	Substantial	Perfect	Substantial
VSD	ECHO-MTD	ECHO-MRI	MRI-MTD
Kappa	1	1	1
Level of agreement	Perfect	Perfect	Perfect
PDA	ECHO-MTD	ECHO-MRI	MRI-MTD
Kappa	0.459	0.459	1
Level of agreement	Moderate	Moderate	Perfect
LVH	ECHO-MTD	ECHO-MRI	MRI-MTD
Kappa	0.688	0.688	1
Level of agreement	Substantial	Substantial	Perfect

Aortic pathology was primarily evaluated qualitatively, using established criteria for describing thoracic aortic anomalies<sup>12,13</sup> and contrasted with the DE outcomes. Comparison was also done between echocardiographic and MRI findings with MTD (considered as gold-standard in this study). Catheterization was only conducted in a small segment of cases, and the findings weren't compared to VENC MR Pressure gradients. This is due to the reason that all patients weren't subjected to the study of "catheter angiographic".

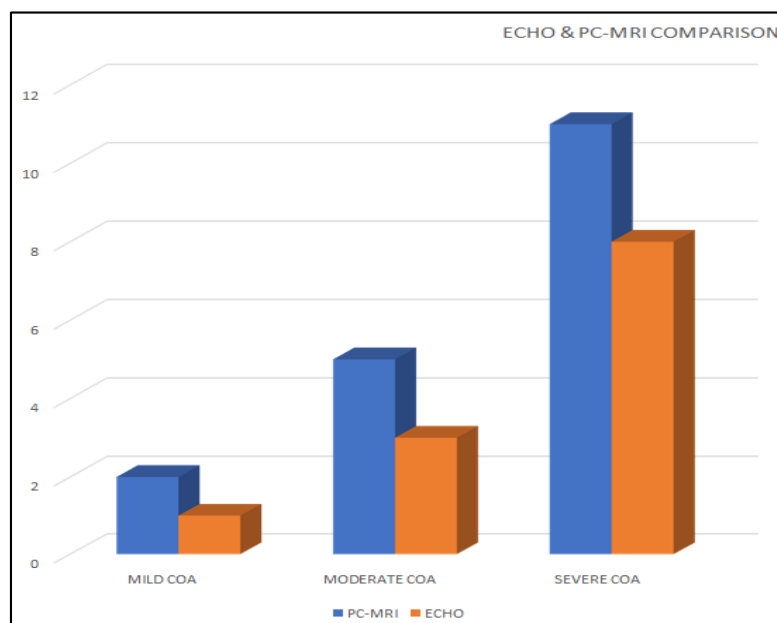


Figure 6. Comparison of echocardiographic and MRI findings

### Statistical Analysis

The observations of the “MULTITEAM DISCUSSION (MTD)” or CCA were used as the gold standard. MRI and echocardiography pressure gradients were compared using linear regression (LR) analysis. Bland & Altman’s method was used to find the mean differences as well as agreement limits. A statistical analysis of inter-modality agreement was also used to compare MRI, echocardiography, as well as MTD (kappa values). All statistical studies were conducted using SPSS statistical software (release 23.0, SPSS Inc.; Chicago, IL).

### Results

This research was performed over a two year period at the DORAI, SKIMS, Srinagar, on patients referred by this concerned department.

During this period, twenty cases with echocardiographic features of CoA/features suspicious for CoA were referred from the department of Cardiology. We analyzed the medical records of twenty patients, twelve of whom were male (sixty percent) and eight of whom were female (forty percent), with a mean age of seventy.

### MRI Findings

Using transverse axial S-E or fast S-E imaging at the level of the AA & AI, it was possible to detect narrowing in nineteen of the twenty-two cases studied. The partial volume effect made it more difficult to demonstrate narrowing on this plane, especially among young kids. Most of the time, this plane showed the tubular hypoplasia of the AA perfectly. It was only possible to show the narrowing in the OCP that encompassed the beginning of the DA.

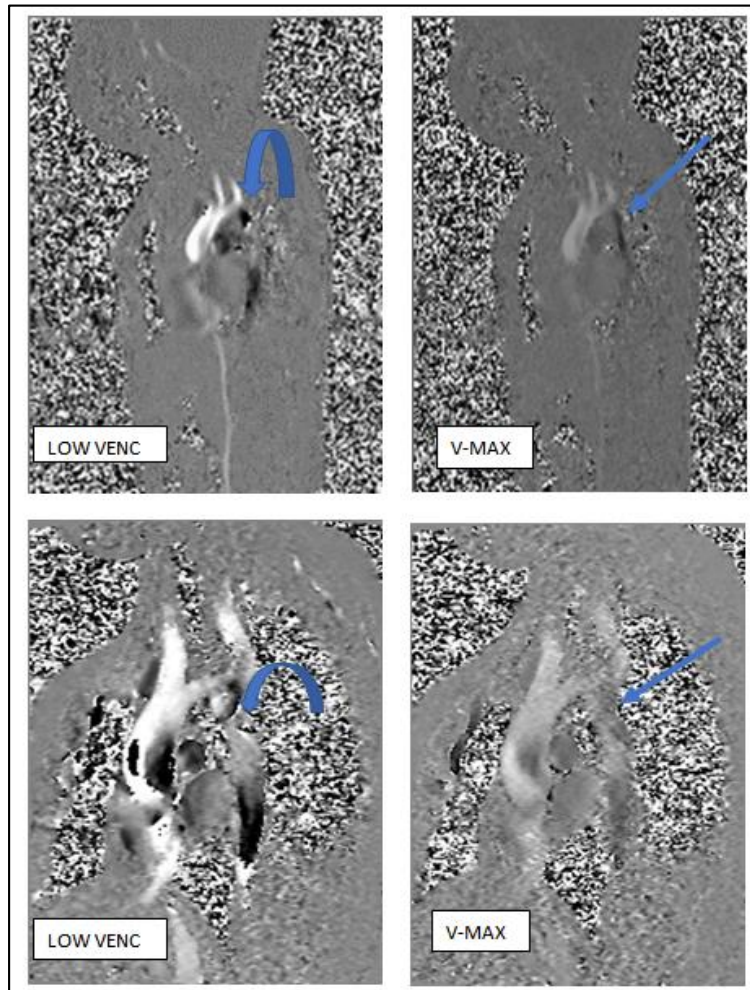


Figure 7. The MR cine diastolic pictures indicate the coarctation location in an OSP (arrows). When the aorta is bent, only parts of the AA can be seen in a single plane (A, B, C)

The coarctation-related narrowing was easier to detect on diastolic images than it was on oblique sagittal cine images. Systolic images, on the other hand, were partly covered by signal voids caused by high-velocity turbulent flow all over the coarctation, which was especially evident on the GE sequences used at the commencement of the research.



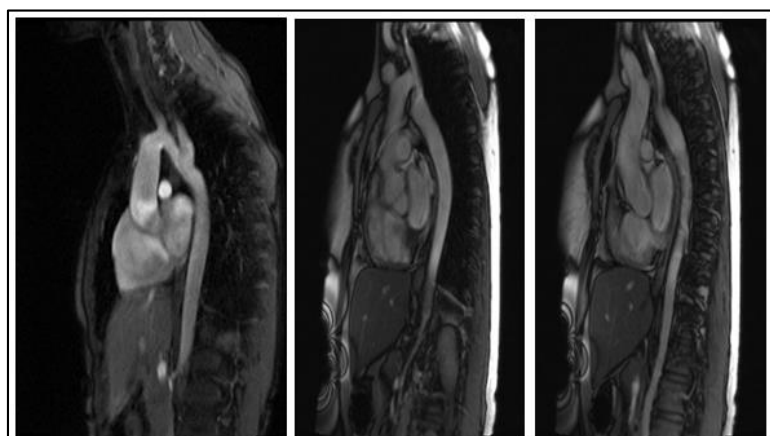


Figure 8. MR cine images in OS systole phase demonstrating coarctation location (arrows)

Some cases may also require the demonstration of collaterals.

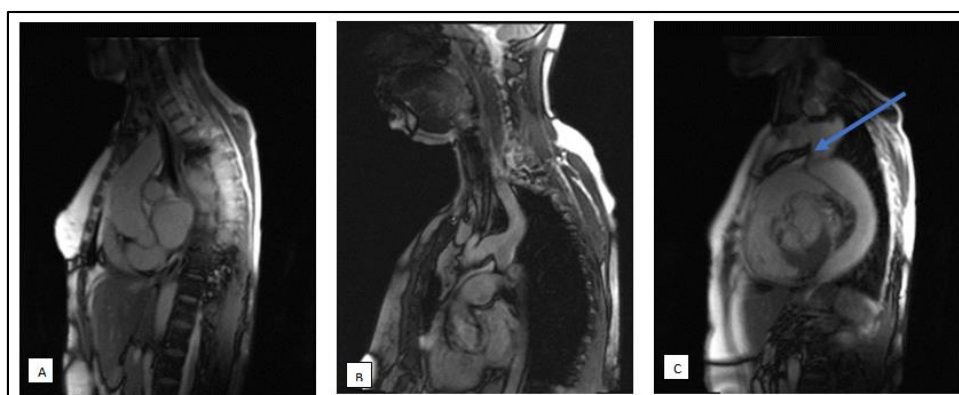


Figure 9. The MR cine diastolic pictures indicate the coarctation location in an OSP (arrows). When the aorta is bent, only parts of the AA can be seen in a single plane (A, B)

Most of the time, the OSP and OCP were the best for directly measuring the increased flow speed in the stenotic jet, which was shown on cine images by VENC sequences. The OSP couldn't determine the jet's max. speed when it was very narrow because of partial volume averaging and the jet moving out of the imaging plane. However, this evaluation could generally be made on the coronal plane.

MR angiography with gadolinium was the best method for capturing the whole TA and its abnormality. The CC was best displayed using oblique MPR as well as volume rendering reconstructions.

### ***CC in response to coarctation severity***

CC evaluation was performed effectively with VENC-MRI by assessing flow of blood in the proximal (ten millimeters below stenosis) as well as distal (at

diaphragm level) portions of the DA. In eleven of the twenty cases, there was strong evidence of CC. In six out of eleven cases with severe stenosis, there was a lot of important CC. CC was present in three of the five moderately stenotic cases.

Table 2  
Calculation of SIG/INSIG CC based on PC-MRI assessment of the severity of COA

No. of Cases	COA Severity (PC-MRI)	CIR. (Distal COA) l/min (A)	CIR. (in DDA AT DL) l/min(B)	FR (A/B)	% (A-B)	CIF	CA
1.	M	0.256	1.63	0.16	537 +		SIG
2.	M	0.637	1.37	0.46	115 +		SIG
3.	Pseudo-coarctation	1.98	1.67	1.19	16-		INSIG
4.	M	0.101	0.265	0.38	162 +		SIG
5.	Unknown	0.474	0.595	0.79	26+		INSIG
6.	Mo	0.146	0.359	0.41	146 +		SIG
7.	Mo	1.55	1.91	0.81	23 +		INSIG
8.	S	2.7	2.63	1.03	2.6 -		INSIG
9.	S	0.121	0.298	0.41	147+		SIG
10.	S	2.21	3.39	0.65	53 +		SIG
11.	Mo	1.61	1.67	0.96	3.7 +		INSIG
12.	S	0.133	0.29	0.46	118+		SIG
13.	S	2.48	1.98	1.25	20 -		INSIG
14.	S	1.28	2.98	0.43	132+		SIG
15.	S	0.135	0.126	1.07	6.6-		INSIG
16.	S	0.163	0.143	1.14	12.3-		INSIG
17.	S	0.21	0.17	1.23	19-		INSIG
18.	S	0.168	0.29	0.76	73+		SIG
19.	Mo	1.89	2.98	0.71	58+		SIG
20.	S	1.77	2.88	0.61	63+		SIG

\*FR - Flow Ratio, CIR - Circulation, CIF - Change In Flow, CA - Collateral Assessment, DL - Diaphragm Level, M - Mild, S - Severe, Mo - Moderate, SIG - Significant, INSIG - Insignificant

- The CoA was short and shelf-like in length.
- In nineteen cases, the position of the narrowing was correctly defined (distal to the left subclavian arteries). In one instance, a specific location of the narrowing wasn't specified because of severe hypoplasia of AA.

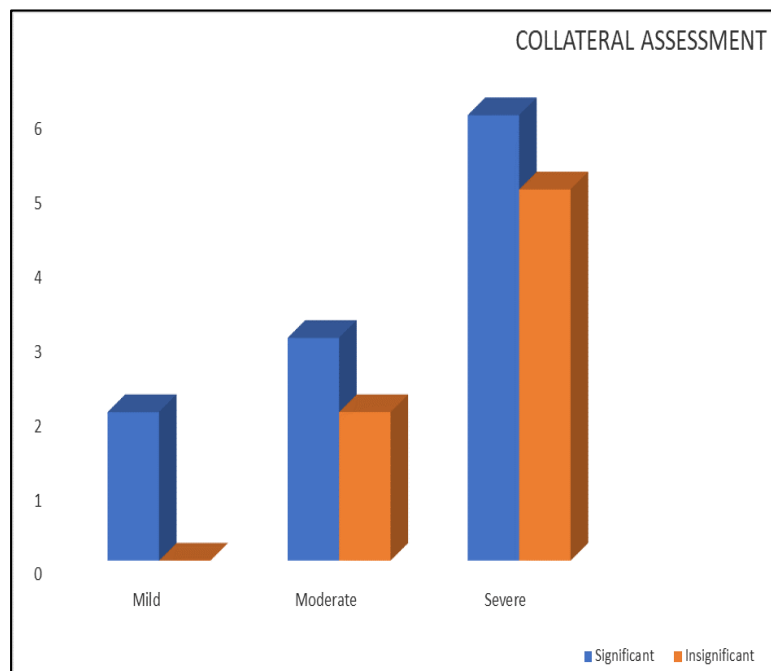


Figure 10. Double column bar diagram for comparison of number of cases with significant and insignificant collateral circulation with increased severity (mild, moderate, and severe) CoA

- The parasagittal view of the coarctation segment was obtained using a combination of TRUFI (True Fast Imaging with Steady-State Free Precession) and HASTE (Half Fourier Acquisition Single Shot Turbo S-E) sequences, along with the MR angiography in different planes. Propofol (Diprivan) was given to sedate kids below six years of age. The ECG signal, respiratory curve, & oxygen levels were all observed using an MR compatible mechanism.
- Images of black blood (BB) were obtained in the axial plane using ECG-gated multi-slice S-E and fast S-E techniques at the beginning. Then, 2 more planes were added that is the coronal as well as OSP, which involved the AA.

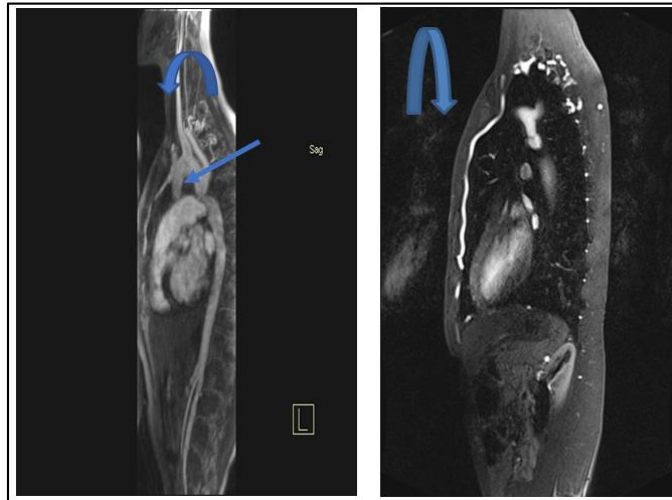


Figure 11. MR image of S-E showing coarctation (arrow) on OSP

This sequence was supplanted in older children as well as adults with a breath-hold turbo S-E BB sequence using a parallel acquisition method that decreased the time of scan while maintaining the relatively similar spatial resolution (SR). The thickness of the slice varied from three to ten mm depending on the size of the patient's heart. A large matrix, like 256x512 in the read direction, was adopted to improve SR without increasing time of acquisition in younger patients.

### ***Associated anomalies or findings spectrum***

Table 3

Tabulated representation of spectrum of associated anomalies/findings

Associated Anomaly/Findings	Echo	MRI	MTD
ASD	3	3	2
VSD	5	5	5
PDA	1	3	3
LVH	6	9	9
PAH	4	8	7
BAV	4	3	3

Tubular hypoplasia of the AA was noticed in 1 situation, PFO was discovered in 2 situations, Shone complex was identified on MTD in 1 situation, and pseudo-CoA ( $\Delta p=12\text{mm Hg}$ ) was detected in 1 situation.

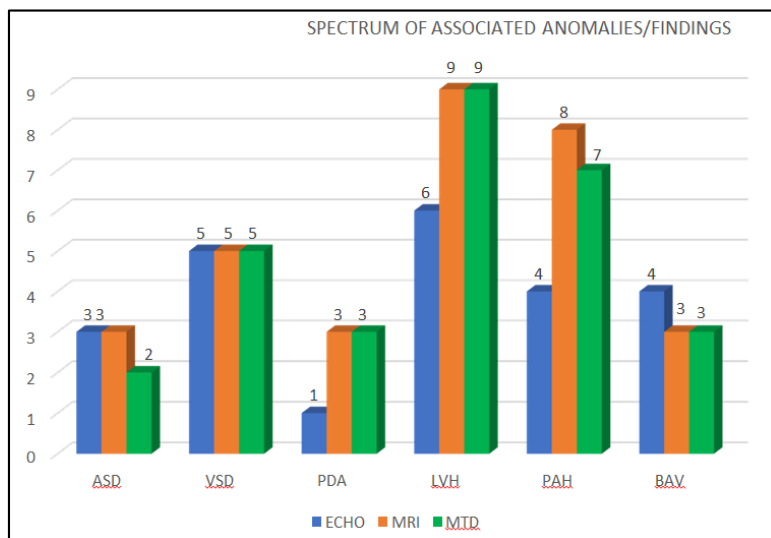


Figure 12. Graphical representation of spectrum of associated anomalies/findings detected in our study

This individual was detected with “Ellis-van Crevald” disorder (homozygous non-sense variability in EXON8 of EVC2 gene).

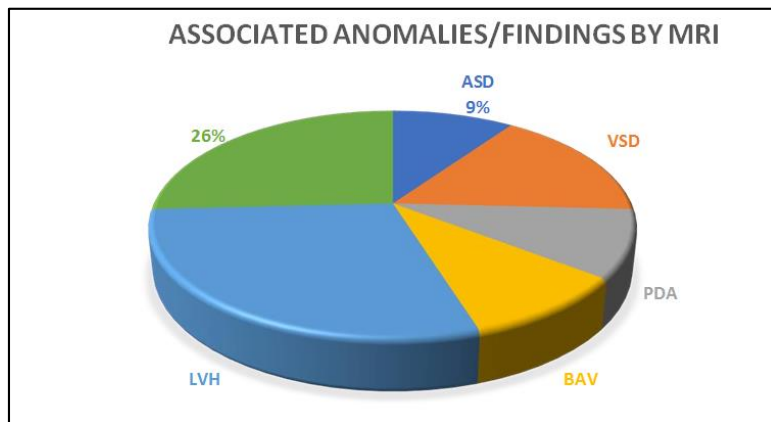


Figure 13. A pie chart depicting the range of anomalies/findings identified by MRI

### ***MRI and de results comparison***

DE was used to diagnose coarctation in seventeen of the twenty patients, and presumption of coarctation and/or AA hypoplasia was brought up in three situations. On echocardiography, the AA or location of coarctation wasn't well shown in three situations. In one of these situations, the echocardiogram showed signs that were skeptical for CoA. When the patient was given a PC-MRI, a treatment of pseudo-coarctation ( $\Delta p=12\text{mmHg}$ ) was done. Thus, this was demonstrated on MTD. In fifteen situations, it was possible to compare VENC-MRI as well as Doppler projections of PG all over the coarctation. PG projections from VENC-MRI are mapped against Doppler projections.

The graph shows a great correlation (correlation coefficient of 0.823 according to Pearson) between the two techniques. As stated above, Doppler measurements were not possible in five situations, and MRI measurements were not possible in single situation. Most of it was caused by a tight stenosis or tubular hypoplasia of the AA, and the large PDA was the main source of blood flow below the coarctation.

## **Discussion**

Cardiac-MRI was performed on patients after an assessment of echocardiographic was conducted for verifying undefined echocardiographic observations, assessment of degree of stenosis (VENC-MRI), better delineation of aortic arch anatomy, accurate delineation of site of coarctation and its relationship to left subclavian artery, measurement of aortic diameters, length of coarctation (short or long segment), associated AA hypoplasia, evaluation of CC and detection of associated anomalies.

In our study, 20 patients with echocardiographic features of/suspicious for CoA were evaluated by Cardiac-MRI, and then the echocardiographic and Cardiac-MRI findings were compared to each other and to the MTD criterion. Our study was supported by research undertaken by Serif Beslic and colleagues at the Institute of Radiology, Clinical Centre University, Sarajevo. This research showed that the outcomes of MRI were 100 percent consistent with clinical as well as echocardiographic observations<sup>14-16</sup>.

Another important research that complements ours was carried out by D. Didier et al. at the Dept. of Radiology, University Hospital of Geneva, to make a comparison the findings of MRI and DE in patients with CoA. Linear regression was used to make comparisons of the PG projections from VENC-MRI and echocardiography (graphical representation). The graphs showed a strong correlation between the 2 techniques ( $r=0.71$ ). To see if the MRI as well as echocardiographic dimensions varied widely, the Bland & Altman method was used to plot the mean values of each pair against each other<sup>17-18</sup>.

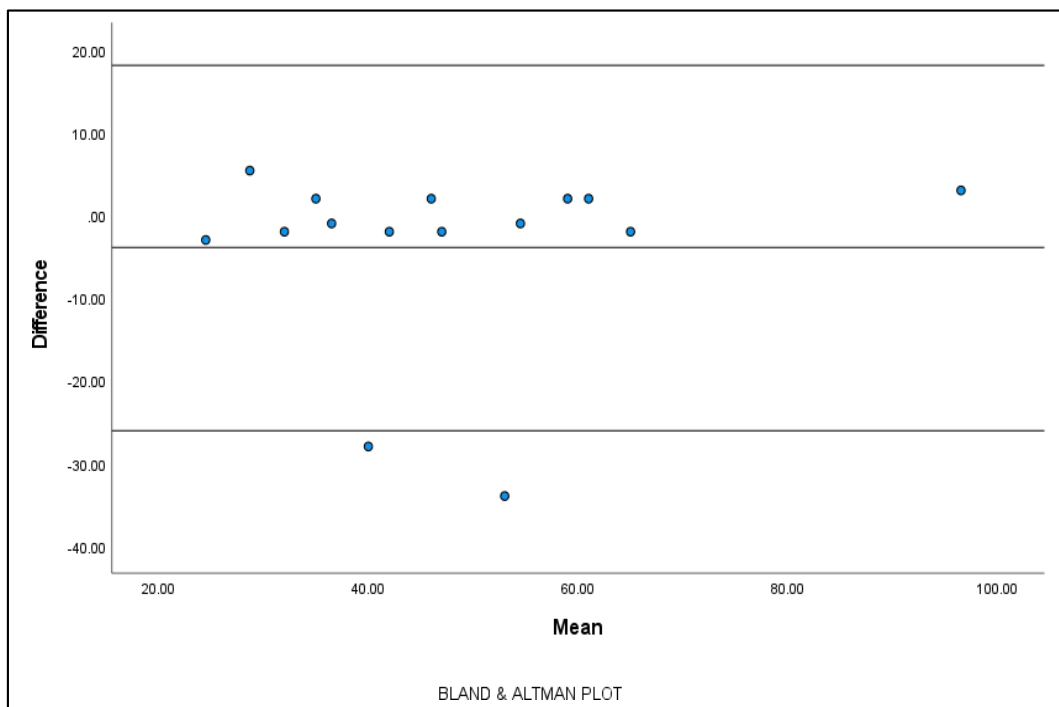


Figure 14. Using the Bland & Altman method, the deviation among Doppler & MRI measurements was shown against the mean value of every pair. The line in the middle shows the average difference, while the lines at the top and bottom show the limits of agreement. ( $\pm 2$  SD).

An MRI study of CoA demonstrated that it was too short in nineteen of twenty patients. Additionally, MRI was adopted to assess the diameters of aortic. While using the measured diameters of aortic, a ratio between both the diameter of the AI and the diameter of the distal DA was calculated, which classified the level of stenosis at the coarctation into 3 groups. In terms of detecting CoA, there was a significant correlation between MRI as well as MTD with a kappa value of 1, along with the moderate correlation between MRI & Echo observations with a KV (kappa value) of 0.459.

Table 4  
Comparison between ECHO & MRI Observations showed moderate correlation between two with kappa value of 0.459

ECHO * MRI Cross tabulation					
Detection of COA			MRI (%)		Total (%)
			0	1	
ECHO	0	Count	1	2	3
		% within ECHO	33.3	66.7	100.0
		% within MRI	100.0	10.5	15.0
	1	Count	0	17	17

		% within ECHO	0.0	100.0	100.0
		% within MRI	0.0	89.5	85.0
Total	Count		1	19	20
	% within ECHO		5.0	95.0	100.0
	% within MRI		100.0	100.0	100.0

SM					
		V	Asymp. SE <sup>a</sup>	Approx. $\tau$ <sup>b</sup>	Approx. Sig.
MoA	Kappa	.459	.305	2.442	.015
N of Valid Situations		20			

\* SM - Symmetric Measures, MoA - Measure of Agreement, SE - Standard Error, V-Value,

In seventeen of the twenty patients who had both an echocardiogram and MRI, the results could be compared. In our research, there was a perfect correlation between the morphological evaluations of echocardiographic as well as MRI observations.

Table 5  
Correlation between PC-MRI and ECHO findings

MRI		ECHO	
MRI	PC	1	.823**
	Sig. (2-tailed)		.000
	N	19	15
ECHO	PC	.823**	1
	Sig. (2-tailed)	.000	
	N	15	15

\* PC - Pearson Correlation

Moreover, the research performed by Serif Beslic et al. at the Institute of Radiology, Clinical Center University, Sarajevo, was related to our findings. This research showed that MRI research findings were completely consistent with clinical as well as echocardiographic observations.

According to our findings, there was substantial CC in cases of CoA that were mild, moderate, or severe. This error might be due to the fact that sample size of our study was small (n=20). This is due the fact that we used only VENC-MRI for the evaluation of collateral circulation which can over-estimate the collateral circulation in mild cases and underestimate in severe cases of CoA.

Hernandez RJ et al. performed a research to evaluate if VENC-MRI could provide understanding into the anatomy and hemodynamics of CC in patients having unrepaired coarctation. For cardiac MRI, 16 cases with discrete coarctation (sixty-



five percent severe, twenty-nine percent mild to moderate) as well as ten controls (median age - 12.0 yrs., range - 9–15) without left-sided CL were sent. Flow volumes (FV) were determined from VENC-MRI images of the diaphragm (distal), coarctation (proximal), as well as the midpoint between the 2 points. For volumes, a means model, repeated-measures assessment was conducted. FV rose by fifty-nine percent ( $p = 0.0002$ ) from the coarctation to the diaphragm in patients with coarctation. This was most noticeable between the proximal as well as midpoint locations by seventy-seven percent ( $p < 0.0001$ )<sup>19</sup>.

To sum up, there was a good correlation between ECHO-MTD, ECHO-MRI, and MRI-MTD when it came to define the spectrum of associated abnormalities. The relatively higher agreement level (KV) between MTD & MRI especially in the identification of PAH & PDA, shows that MRI is a better imaging method for identifying problems that are linked to CoA.

## References

1. Beigelman-Aubry C, Badachi Y, Akakpo JP, Lenoir S, Gamsu G, Grenier PA. Practical morphologic approach to the classification of anomalies of the aortic arch. *Eur Radiol.* 2002;12;Suppl 1:391-6.
2. Weissleder R, Wittenberg J. *Diagn Imaging.* 1994;94-6.
3. Marchal G, Bogaert J. Non-invasive imaging of the great vessels of the chest. *Eur Radiol.* 1998;8(7):1099-105. doi:10.1007/s0033 00050516, PMID 9724420.
4. Bogaert J, Kuzo R, Dymarkowski S, Janssen L, Celis I, Budts W, et al. Follow-up of patients with previous treatment for coarctation of the thoracic aorta: comparison between contrast-enhanced MR angiography and fast spin-echo MR imaging. *Eur Radiol.* 2000; 10(12):1847-54.
5. Gurney JW, Winer-Muram HT. Aortic anomalies. In: *Pocket radiologist. chest.* Salt Lake City: Amirsys Inc. 2003; p. 284-6.
6. Webb WR, Higgins CB. *Thoracic Imaging. Radiography of congenital heart disease.* ISBN: 1605479764.
7. Rasalingam R, Makan M, Perez JE. *The Washington manual of echocardiography.* 2012; ISBN: 9781451113402.
8. Julsrud PR, Breen JF, Felmlee JP, Warnes CA, Connolly HM, Schaff HV. Coarctation of the aorta: collateral flow assessment with phase-contrast MR angiography. *AJR Am J Roentgenol.* 1997 Dec;169(6):1735-42. doi:10.2214/ajr.169.6.9393200, PMID 9393200.
9. Schintz HR, Baensch WE, Friedl E, Wehlinger E, Holzmann M. *Traite de radio diagnostic. Le thorax. Vol. 3.* Neuchatel: Delachaux- Niestle SA. 1957;p. 2950-3.
10. Glancy DL, Morrow AG, Simon AL, Roberts WC. Juxtaductal aortic coarctation. Analysis of 84 patients studied hemodynamically, angiographically, and morphologically after age 1 year. *Am J Cardiol.* 1983;51(3):537-51.
11. Bogaert J, Kuzo R, Dymarkowski S, Janssen L, Celis I, Budts W, et al. Follow-up of patients with previous treatment for coarctation of the thoracic aorta: comparison between contrast-enhanced MR angiography and fast spin-echo MR imaging. *Eur Radiol.* 2000; 10(12):1847-54

12. Pinzon JL, Burrows PE, Benson LN, Moës CA, Lightfoot NE, Williams WG, et al. Repair of coarctation of the aorta in children: postoperative morphology. *Radiology*. 1991;180(1):199-203.
13. Bogaert J, Gewillig M, Rademakers F, Bosmans H, Verschakelen J, Daenen W, et al. Transverse arch hypoplasia predisposes to aneurysm formation at the repair site after patch angioplasty for coarctation of the aorta. *J Am Coll Cardiol*. 1995;26(2):521-7.
14. Kramer U, Dammann F, Breuer J, Sieverding L, Claussen CD. Cardiac imaging in infants with aortic isthmus stenosis: A comparison of contrast enhanced MRA and a high-resolution 3D double Slab technique. *Eur Radiol*. 2002;12:295-6.
15. Bonomo B. Spiral CT vs MR in aortic diseases ECR. *Eur Radiol*. 2000;10;Suppl 1:28.
16. FA: Mohammed, R. A., Saifaddin, A. L., Mahmood, H. F., & Habibi, N. (2022). Seismic Performance of I-shaped Beam-column Joint with Cubical and Triangular Slit Dampers Based on Finite Element Analysis. *Journal of Studies in Science and Engineering*, 2(1), 17-31.
17. Kumar, S. (2022). A quest for sustainium (sustainability Premium): review of sustainable bonds. *Academy of Accounting and Financial Studies Journal*, Vol. 26, no.2, pp. 1-18
18. Allugunti, V.R. (2019). Diabetes Kaggle Dataset Adequacy Scrutiny using Factor Exploration and Correlation. *International Journal of Recent Technology and Engineering*, Volume-8, Issue-1S4, pp 1105-1110.